

1 **Dose Estimates of an Early 20<sup>th</sup> Century Kilovoltage Radiotherapy Treatment for**  
2 **the Potential Application to Viral Pneumonia Using Modern X-Ray Equipment**

3 D. Roa<sup>1\*</sup>, H. Moyses<sup>1</sup>, S. Leon<sup>2</sup>, B. Hamrick<sup>3</sup>, G. Sarria<sup>4</sup>, B. Li<sup>5</sup>, T. Tajima<sup>6</sup>, A. Necas<sup>7</sup>, C. Guzman<sup>8</sup>, O.  
4 Paucar<sup>9</sup>, A. Gonzales<sup>10</sup>, R. Chalco<sup>10</sup>, M. Montoya<sup>10</sup>, Z. Arque<sup>10</sup>, A. Gonzales<sup>11</sup> and J. Hernandez<sup>12</sup>

5 **\*Corresponding author:**

6 **Dante E. Roa**

7 [droa@uci.edu](mailto:droa@uci.edu)

8 <sup>1</sup>Department of Radiation Oncology, University of California, Irvine Health, Orange, CA 92868

9 <sup>2</sup>Department of Radiology, University of Florida, Gainesville, FL 32610

10 <sup>3</sup>Environmental Health and Safety, University of California, Irvine Health, Orange, CA 92868

11 <sup>4</sup>Department of Radiation Oncology, University Medical Center Mannheim, Medical Faculty Mannheim,  
12 Heidelberg University, Mannheim, Germany

13 <sup>5</sup>Department of Radiation Oncology, University of California, San Francisco, CA 94115

14 <sup>6</sup>Department of Physics and Astronomy, University of California, Irvine, CA 92697

15 <sup>7</sup>TAE Technologies, 1961 Pauling, Foothill Ranch, CA 92610

16 <sup>8</sup>Facultad de Ciencias Naturales y Matematica, Universidad Nacional Federico Villarreal – Lima, Peru

17 <sup>9</sup>Facultad de Ingenieria Electrica y Electronica, Universidad Nacional de Ingenieria – Lima, Peru

18 <sup>10</sup>Facultad de Ciencias, Universidad Nacional de Ingenieria – Lima, Peru

19 <sup>11</sup>Clinica Aliada contra el Cancer – Lima, Peru

20 <sup>12</sup>HRS Oncology International, Las Vegas, NV 89119

21

22 **Abstract**

23 Purpose: To simulate an early 20<sup>th</sup> century radiotherapy pneumonia treatment to evaluate the viability  
24 of using modern fluoroscopes to deliver a low-dose single-fraction treatment to the lungs and to  
25 compare calculated organ doses to current tolerance guidelines.

26 Materials and Methods: PENELOPE v.2008 was used to simulate a 1920s-40s radiotherapy treatment to  
27 both lungs of pneumonia patients using a modern beam quality. Organs-at-risk were: skin, breasts,  
28 esophagus, ribs, vertebrae, heart, thymus and spinal cord. A 100 kV<sub>p</sub> beam with 3 mm Al HVL, 25 x 25  
29 cm<sup>2</sup> posterior-anterior field and 50 cm source-to-surface distance were used. Simulations had a  
30 resolution of 0.4 x 0.4 x 0.06 cm<sup>3</sup> and a 6% uncertainty. 100% dose was normalized to the skin surface  
31 and results were displayed in axial, coronal and sagittal planes. Dose volume histograms were generated  
32 in MATLAB for further analysis. Prescriptions of 0.3, 0.5 and 1.0 Gy were applied to the 15% isodose line  
33 for organ dose comparison to modern tolerances.

34 Results: Right and left lung volumes were well-covered by the 15% isodose (95% and 97%, respectively).  
35 Mean doses were: lungs 28% (right) 29% (left), breasts 6% (right and left), skin 16%, esophagus 16%, ribs  
36 66%, vertebrae 55%, heart 11%, thymus 5% and spinal cord 22%. For all prescriptions, absolute  
37 maximum skin doses were above the transient erythema threshold (2.0 Gy), while lungs were below  
38 pneumonitis (6.5 Gy) and fibrosis (30.0 Gy) thresholds. For 0.5 and 1.0 Gy prescriptions, maximum heart  
39 doses were above the 0.5 Gy ICRP-recommendation. Maximum doses to other organs were below  
40 modern dose thresholds.

41 Conclusion: All prescriptions normalized to the 15% isodose line would have resulted in lung doses  
42 without risk of complications. Skin and heart maximum doses could have reached detriment thresholds,  
43 particularly for the 1.0 Gy prescription. Equal-or-better treatments should be possible with a modern  
44 fluoroscope.

45 Keywords: radiotherapy, pneumonia, kilovoltage x-rays, low dose, fluoroscopes, c-arm

46

## 47 **Introduction**

48 In the early 20<sup>th</sup> century, viral and bacterial pneumonia patients were treated with radiotherapy  
49 to deliver lung doses of 0.3-1.0 Gy using 100-200 kV<sub>p</sub> x-ray beams. This was a one-time  
50 treatment and signs of recovery appeared as early as 3-5 hours after irradiation. Radiotherapy  
51 treatments stopped in the 1940s with the advent of antibiotic- and steroid-therapies despite  
52 their high cure rate.<sup>1</sup> However, the potential to use radiotherapy for the treatment of viral  
53 pneumonia has been suggested in modern times and is an area of research for treating COVID-  
54 19 patients.<sup>1-3</sup> Modern fluoroscopes could deliver therapeutic radiation doses to the lungs  
55 using x-ray energies similar to those used historically, and they are more widely available than  
56 radiotherapy linear accelerators.

57 It is worth exploring the dosimetry that a historical pneumonia treatment could have achieved  
58 via computer simulations using a kV x-ray beam on an anthropomorphic phantom.

59 Reproduction of a beam quality of the era would have required a detailed description of  
60 materials, dimensions and design of a 1920s-40s x-ray source, which is not readily available.

61 Therefore, a modern x-ray tube with minor modifications was used, which can lead to an  
62 experimental verification with existing systems in the future. Prescription dose information can  
63 be extracted from published clinical and historical reports<sup>1-6,9-12</sup> and used in the simulations.

64 In this study, prescription doses of 0.3, 0.5 and 1.0 Gy were used for isodose normalization  
65 while dose distributions and maximum doses to critical organs were evaluated according to

66 modern dose tolerance guidelines. Results from this work and potential implementation using  
67 modern fluoroscopes are presented.

68

## 69 **Materials and Methods**

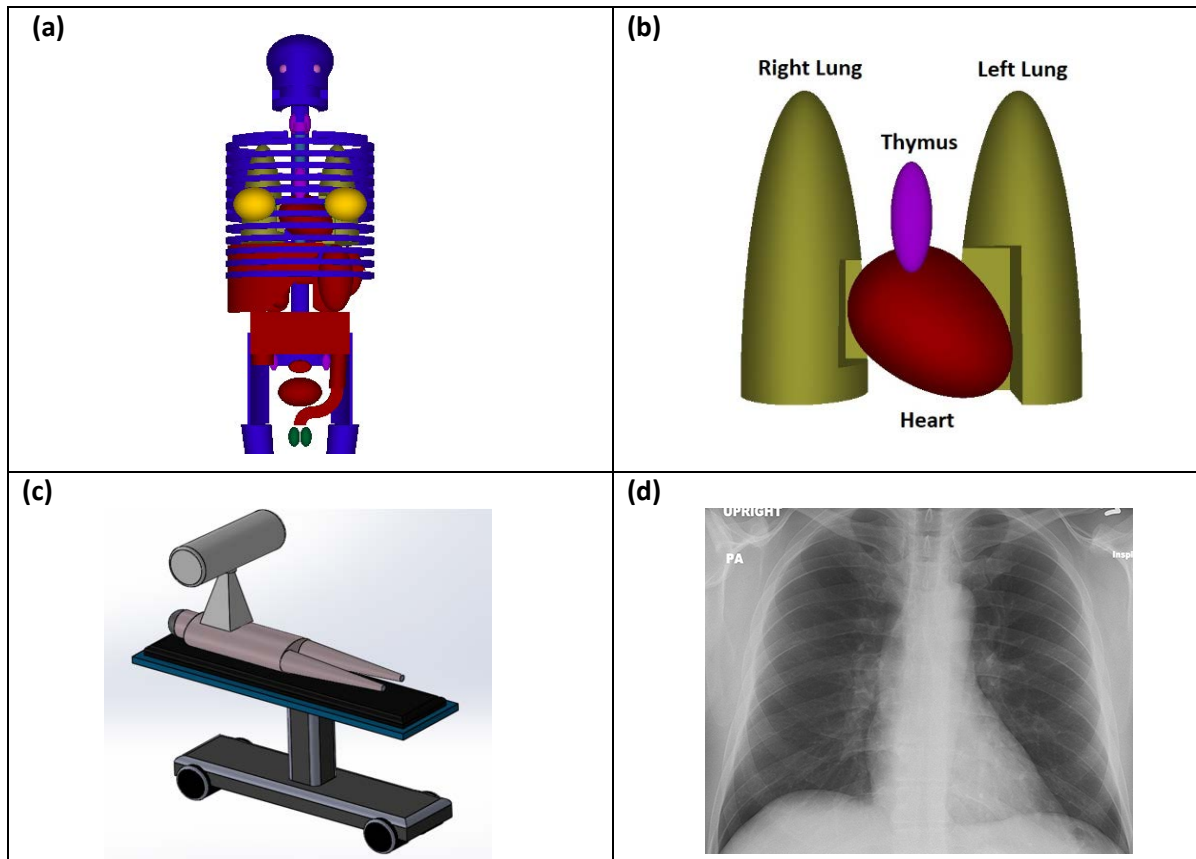
70 PENELOPE with its mathematical anthropomorphic phantom was used for Monte Carlo (MC)  
71 simulations.<sup>7</sup> The phantom was an adult female anatomy that included most organs (Fig. 1a-b)  
72 with published density information for each of them. Each lung was 24 cm superior-inferior, 12  
73 cm left-right and 10 cm anterior-posterior. Organs-at-risk were: skin, breasts, ribs, esophagus,  
74 vertebrae, heart, thymus and spinal cord. Skin volume was limited to the thoracic region only.

75 SPEKTR 3.0<sup>8</sup> was used to generate a 100 kV<sub>p</sub> x-ray beam spectrum from a tungsten target with  
76 an aluminum filter. Historically, a single- or three-phase generator<sup>5</sup> would have produced  
77 significant ripple and a lower effective energy than a modern beam; however, 100 kV<sub>p</sub> is at the  
78 bottom of the cited energy range, so the effective energy should still be appropriate for the  
79 historical context. A report of that time recommends the use of a 3-mm Al filter for x-ray  
80 radiotherapy of the lungs,<sup>9</sup> which would result in a half-value layer (HVL) of approximately 3  
81 mm Al, assuming an inherent tube filtration similar to modern tubes and tube ripple  
82 appropriate for a 3-phase generator<sup>1</sup>. Thus, a 3 mm Al HVL was selected for the simulated  
83 beam, which is a slightly softer spectrum than on modern units.<sup>10</sup>

---

<sup>1</sup> Calculated using IPEM 78 Spectrum Processor Version 3.0. The Institute of Physics and Engineering in Medicine. 2015

84 The simulated treatment consisted of a 25 x 25 cm<sup>2</sup> posterior-anterior (PA) field at 50 cm  
85 source-to-surface distance (SSD) (Fig. 1c). The field covered both lungs and could have been



86 **Figure 1.** (a) PENELOPE's mathematical anthropomorphic phantom of a female anatomy. (b) Thoracic  
87 anatomy inside the phantom. (c) Posterior-anterior treatment field used in the simulations. (d)  
88 Posterior-anterior tuberculosis chest x-ray during the first world war.<sup>11</sup>

89

90 defined with an x-ray system of that time (Fig. 1d) which was used for radiography, fluoroscopy  
91 and radiotherapy procedures.<sup>4-6,9,11,12</sup>

92 The simulations had a spatial resolution of 0.4 x 0.4 x 0.06 cm<sup>3</sup> and an uncertainty of 6% for 2 x  
93 10<sup>9</sup> histories. Cumulative dose volume histograms (DVHs) were generated in MATLAB  
94 (MathWorks, Natick, MA) and the MATLAB DVH code was validated using a known data set

95 prior to the actual data analysis. DVHs were generated for the left/right lungs, skin, left/right  
96 breasts, esophagus, ribs, vertebrae, heart, thymus and spinal cord.

97 The skin surface dose corresponded to 100% and was the reference dose calibration location.

98 The 15% isodose was normalized to a 0.3, 0.5 and 1.0 Gy prescription dose to extract absolute

99 dose information. Mean and maximum relative doses for each organ-at-risk were extracted

100 from the DVHs, normalized to each prescription dose, and evaluated against the International

101 Commission on Radiological Protection (ICRP) and other reports for organ dose tolerance

102 assessment.<sup>13-22</sup>

103

## 104 **Results**

105 Figure 2a shows the percent depth dose (PDD) at the phantom's central sagittal plane. Peak

106 doses at 0.5, 3.0, 5.5, and 19.5 cm depths corresponding to ribs or vertebrae regions resulted

107 from photoelectric interactions. The most prominent peak was in the ribs at 0.5 cm depth with

108 a 325% maximum point dose. The second-most prominent was in the vertebrae at 3 cm depth

109 with 225% maximum dose. Conversely, soft tissue regions showed a smooth dose deposition

110 reduction as a function of depth.

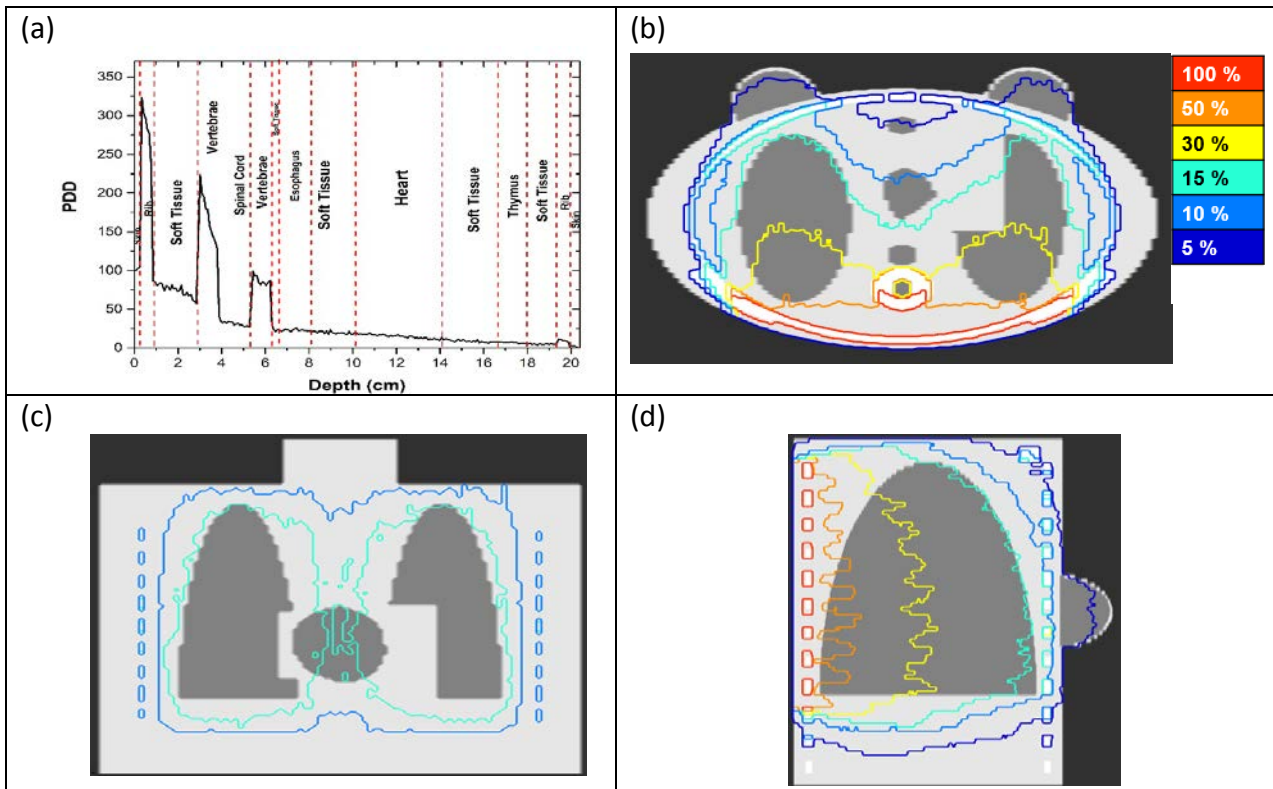
111 Figures 2b-2d show axial, coronal and sagittal isodoses. The 15% isodose provided coverage to

112 both lungs with 95% and 97% of the right and left lung volumes covered as shown in the DVH

113 (Fig 3a). The peak doses to the lungs were 72% (right) and 73% (left) of the maximum dose.

114 Table 1 shows mean and maximum absolute doses for the lungs, skin, breasts, esophagus, ribs,

115 vertebrae, heart, thymus and spinal cord, after applying a 0.3, 0.5 and 1.0 Gy prescription dose



116 **Figure 2.** Percent depth dose with 100% at the skin surface (a) and dose distribution displayed in the axial  
 117 (b), coronal (c) and sagittal (d) planes. The 15% isodose (cyan) distribution provided an effective dose  
 118 coverage to both lungs.

119

120 normalization to the 15% isodose, as well as dose tolerances provided by ICRP and other  
 121 reports. The maximum dose to the skin exceeded 2 Gy<sup>13-15</sup> (the transient erythema dose  
 122 threshold) by 44%, 240%, and 480% for the 0.3, 0.5, and 1.0 Gy prescriptions, respectively. The  
 123 heart maximum dose exceeded 0.5 Gy (the threshold for potential cardiovascular and blood  
 124 circulatory effects) by 5%, 76%, and 352% for the 0.3, 0.5, and 1.0 Gy prescriptions,  
 125 respectively.<sup>13,15,16</sup> The heart mean dose also exceeded this threshold by 42% for the 1.0 Gy  
 126 prescription, while it remained below the threshold for the 0.3 Gy and 0.5 Gy prescriptions.

127 Maximum doses to the lungs did not pose any risk for pneumonitis (6.5 Gy threshold for acute  
 128 exposure)<sup>13,17</sup> or fibrosis (30.0 Gy threshold)<sup>17</sup> for any prescription dose. The lung mean doses

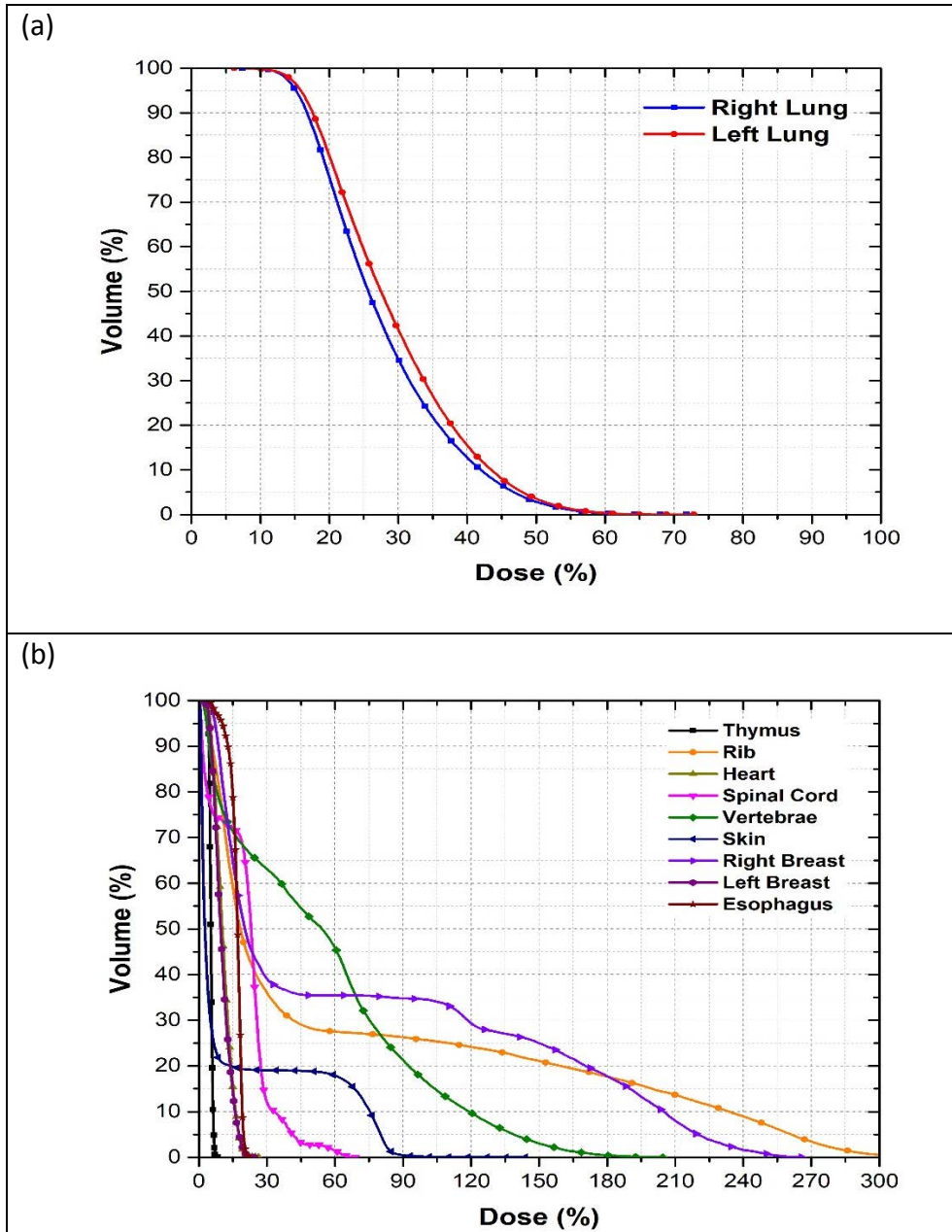


**Figure 3.** Cumulative dose volume histograms for the right/left lungs (a) and organs at risk (b).

129

130 suggested a prescription dose normalization to the 20% instead of the 15% isodose could be used  
 131 which would result in lower doses to critical organs. Mean and maximum doses to the breast were  
 132 below the proposed 1.0 Gy dose threshold at which the risk for developing secondary cancers  
 133 increases in women younger than 40 years.<sup>18</sup>

134



**135Table 1.** Mean and maximum relative and absolute doses are shown for prescription doses of 0.3, 0.5 and 1.0 Gy normalized to the 15% isodose line and compared to modern dose tolerance data.

Organ	Relative Dose		0.3 Gy prescription		0.5 Gy prescription		1.0 Gy prescription		Modern Dose Tolerances (Gy)
	Mean (%)	Max (%)	Mean (Gy)	Max (Gy)	Mean (Gy)	Max (Gy)	Mean (Gy)	Max (Gy)	
Right Lung	27.6	71.8	0.55	1.44	0.92	2.40	1.84	4.79	6.5 <sup>13</sup> (pneumonitis) 30.0 <sup>17</sup> (fibrosis)
Left Lung	29.0	72.8	0.58	1.46	0.97	2.43	1.93	4.86	
Skin	16.3	144.0	0.33	2.88	0.54	4.80	1.09	9.60	2.0 <sup>14</sup> (transient erythema)
Right Breast	5.6	12.6	0.11	0.25	0.19	0.42	0.37	0.84	1.0 Gy < For < age 40 2.5 fold risk <sup>18</sup> For age 40 <, no excess risk <sup>18</sup>
Left Breast	6.3	12.4	0.13	0.25	0.21	0.41	0.42	0.83	
Ribs	66.4	324.0	1.33	6.48	2.21	10.80	4.43	21.60	< 30.0 Gy <sup>21,22</sup> single fraction 22.0 Gy for < 1 cc
Vertebrae	54.8	204.5	1.10	4.09	1.83	6.82	3.65	13.64	12.4-14.0 <sup>21,22</sup> single fraction
Heart	10.6	26.3	0.21	0.53	0.35	0.88	0.71	1.76	0.5 <sup>13,15</sup> 3.0-4.0 <sup>16</sup>
Thymus	5.3	8.4	0.11	0.17	0.18	0.28	0.35	0.56	0.71 <sup>20</sup>
Spinal Cord	20.3	69.1	0.41	1.38	0.68	2.30	1.35	4.60	7.0 <sup>21,22</sup> single fraction
Esophagus	16.4	22.4	0.33	0.45	0.55	0.75	1.09	1.50	40.0-45.0 <sup>19</sup> (acute esophagitis) < 34.0 <sup>22</sup> (mean dose)

137 Ribs maximum doses (prescription dose) were 78% (0.3 Gy), 64% (0.5 Gy) and 28% (1.0 Gy)  
138 below the 30.0 Gy single-fraction dose threshold. Furthermore, the dose to 1 cm<sup>3</sup> of the ribs'  
139 volume, for all prescriptions, was below the 22.0 Gy single-fraction dose threshold.<sup>21,22</sup> The  
140 vertebrae maximum doses (prescription dose) were 67% (0.3 Gy) and 45% (0.5 Gy) below, but  
141 11% (1.0 Gy) above the 12.4 Gy single-fraction dose threshold.<sup>21,22</sup> Ribs and vertebrae  
142 maximum doses for all prescriptions far exceeded the ICRP 118 recommended limit of 2.0 Gy  
143 dose per fraction but not the cumulative dose limit of 50.0 Gy.<sup>13</sup> Mean and maximum doses to  
144 other critical organs for all prescription doses were well within modern dose tolerances.

145

## 146 **Discussion**

147 Calabrese et al.,<sup>1</sup> were the first to suggest re-visiting the role of radiotherapy to treat  
148 pneumonia and now, this suggestion has a newfound relevance in light of the COVID-19  
149 pandemic. Early animal experiments demonstrated that low radiation doses upregulated  
150 lymphocytosis and reduced inflammation.<sup>1,2,27,28</sup> Today, modern studies support these  
151 conclusions.<sup>29,30</sup> This investigative dosimetric analysis provides quantitative information on  
152 dose distributions and detriments to organs from such radiation treatments and suggests a  
153 potential treatment delivery with bedside c-arm fluoroscopes in an inpatient setting.

154 For a simple treatment setup consisting of a PA field, the 15% isodose provided effective  
155 coverage to the lungs with 95% and 97% of the right and left lung volumes covered. After  
156 applying a 0.3, 0.5 or 1.0 Gy prescription dose to the 15% isodose, the maximum dose to the  
157 lungs did not exceed modern thresholds for pneumonitis or fibrosis.<sup>13,17</sup> However, it could have

158 exacerbated pre-radiation fibrosis caused by the pneumonia and/or affected patients with  
159 borderline interstitial fibrosis.

160 For the 0.3 and 0.5 Gy prescriptions, the resulting 2.0-5.0 Gy skin dose may produce signs of  
161 transient erythema within two weeks after exposure, recoverable epilation within eight weeks,  
162 and no observable effects after 40 weeks.<sup>14</sup> For skin doses of 5.0-10.0 Gy, expected from a 1.0  
163 Gy prescription, transient erythema could manifest within two weeks, possible prolonged  
164 erythema and permanent epilation within eight weeks, and at the upper end of the dose range,  
165 dermal atrophy and induration after 40 weeks.<sup>14</sup> It is likely that for the 0.3 and 0.5 Gy  
166 prescriptions, detrimental skin effects would not be permanent, but that may not be the case  
167 for a 1.0 Gy dose.

168 The 0.5 and 1.0 Gy prescriptions had maximum doses to the heart that significantly exceeded  
169 the 0.5 Gy dose threshold for possible cardiovascular and blood circulatory effects according to  
170 the ICRP 118 report.<sup>13</sup> The ICRP 120 report<sup>15</sup> supports the 0.5 Gy threshold statement;  
171 however, it adds that some uncertainty remains at this threshold. Other studies suggest that  
172 the risk of radiation-related heart disease from a low dose radiotherapy can begin to manifest  
173 at 3.0-4.0 Gy.<sup>16</sup> It is possible that a maximum heart dose of 0.9 Gy (0.5 Gy prescription) or 1.8  
174 Gy (1.0 Gy prescription) could cause microvascular damage to the myocardium, however, the  
175 risk for heart-related complications would be low. Furthermore, peak skin doses from modern  
176 interventional cardiac procedures routinely exceed 2.0-3.0 Gy,<sup>23</sup> which implies that cardiac  
177 doses over 0.5 Gy are frequent and not an impediment to treatment. The 0.3 Gy prescription  
178 did not exceed this limit.

179 Maximum doses to the ribs and vertebrae for all prescriptions were below dose thresholds for a  
180 single fraction treatment.<sup>21,22</sup> However, they far exceeded ( $\geq 200\%$ ) the recommended ICRP 118  
181 fractionated dose of 2.0 Gy.<sup>13</sup> Although the risk of radionecrosis, rib fracture, and/or  
182 musculoskeletal atrophy would be low, no additional treatments without risk of complications  
183 would be possible with this setup. Additional treatment fields, such as anterior-posterior (AP)  
184 or laterals, could reduce maximum doses to these structures, but not below 2.0 Gy at the  
185 higher prescribed doses.

186 Published reports indicate that women under the age of 40 could have a 2.5-fold greater risk of  
187 secondary cancers if exposed to a dose greater than 1.0 Gy, compared to no risk for older  
188 women 10 years after irradiation.<sup>18</sup> In this work, median doses to the breasts were below this  
189 level suggesting little-to-no detrimental effects. Maximum doses to the spinal cord, esophagus  
190 and thymus were within modern dose tolerances and did not pose risk of future detriment.<sup>13,19-  
191 22</sup>

192 This study indicates that a radiotherapy pneumonia treatment with a PA field and a 0.3 or 0.5  
193 Gy prescription dose to both lungs would have a low probability of radiation-induced detriment  
194 to critical organs. However, a 1.0 Gy dose treatment might be problematic. Treatment setups  
195 employing more fields could result in a more homogeneous dose distribution to the lungs, and  
196 lower dose to critical organs; this is an area of future work.

197 Treatment setups with two or more fields and hardened beams are possible with modern  
198 fluoroscopes. Fixed interventional c-arms could be ideal due to their large, highly-filtered x-ray  
199 beams, higher x-ray tube heat capacities, and ease of positioning. Mobile c-arms could also be  
200 used for this purpose, albeit with longer treatment times but with the convenience of an in-situ

201 treatment delivery. Modern fluoroscopes do not have field sizes as large as those simulated,  
202 however, therapy covering the entire lung field is possible with multiple beam angles.

203 A modified fluoroscopy unit with a larger field size might be possible with manufacturer  
204 support . While such a system may not be legally used for imaging in the U.S., it could  
205 potentially be used as an investigational device under IRB approval. Perhaps another option  
206 could be the use of existing fluoroscopes on targeted treatments to affected areas identified on  
207 CT.<sup>24</sup>

208 The prospect of rapid, inexpensive, and non-invasive therapy to reduce or prevent ventilator  
209 requirements could be invaluable and even paradigm-changing for centers with limited  
210 ventilator supplies. Clinical trials to evaluate the efficacy of low-dose radiation with linear  
211 accelerators for COVID-19 patients are underway in India, Iran, Italy, Spain, and U.S. However,  
212 there are no trials exploring the use of a c-arm based delivery.

213 Low dose treatments (0.3-0.5 Gy) via mobile c-arm fluoroscope in-situ (e.g. at the patient  
214 bedside in intensive care units or emergency rooms) could prevent viral spread, contamination  
215 of radiotherapy clinics and other hospital spaces, and could be cost effective. The benefit-to-  
216 risk ratio is especially high for the elderly patients, who are more susceptible to complications  
217 from COVID-19 and less likely to develop radiation-induced cancers<sup>25</sup>. Whereas the  
218 radiobiologic response remains to be explored further in COVID-19 pneumonia<sup>26</sup>, the  
219 implementation of a safe, illness-reducing therapy delivered with c-arm technology could be  
220 immediately implemented. Patients in low- to middle-income countries could have access to a  
221 viable life-saving treatment until a more definitive cure becomes available.

222

## 223 Acknowledgements

224 The authors would like to thank Professor Mauro Valente of the University of Cordoba,  
225 Argentina for his support with the Monte Carlo simulations. We also would like to extend our  
226 gratitude to Mr. Johnny Drake and Dr. Ron Villane from Ziehm Imaging as well as Dr. Jon Lea  
227 from GE Healthcare for useful technical discussions and support for this work.

228 No financial support was received for this project.

229

## 230 References

- 231 1. Calabrese EJ and Dhawan G. How radiotherapy was historically used to treat pneumonia:  
232 could it be useful today? Yale Jour. Biol. and Med. 2013; 86, 555-570.
- 233 2. Kirkby C and Mackenzie M. Is low dose radiation therapy a potential treatment for COVID-  
234 19 pneumonia? Radiotherapy and Oncology. 2020;  
235 [https://doi.org/10.1016/j\\_radonc.2020.04.004](https://doi.org/10.1016/j_radonc.2020.04.004)
- 236 3. Dhawan G, Kapoor R, Dhawan R, et al. Low dose radiation therapy as a potential life-saving  
237 treatment for COVID-19-induced acute respiratory distress syndrome (ARDS). Radiotherapy  
238 and Oncology. 2020; [https://doi.org/10.1016/j\\_radonc.2020.05.002](https://doi.org/10.1016/j_radonc.2020.05.002)
- 239 4. Haus AG and Cullinan JE. Screen film processing systems for medical radiography: A  
240 historical review. RadioGraphics. 1989; 9(6):1203-1224.
- 241 5. Krohmer JS. Radiography and fluoroscopy, 1920 to the present. RadioGraphics. 1989;  
242 9(6):1129-1153.
- 243 6. Mould RF. The early history of x-ray diagnosis with emphasis on the contributions of physics  
244 1895-1915. Phys. Med. Biol. 1995; 40:1741-1787.

- 245 7. Sempau J, Badal A and Brualla L. A PENELOPE-based system for the automated Monte Carlo  
246 simulation of clinacs and voxelized geometries - application for far-from-axis fields. Med.  
247 Phys. 2011; 38, 5887–5895.
- 248 8. Punnoose J, Xu J, Sisniega A, et al. Technical note: SPEKTR 3.0 – A computational tool for x-  
249 ray spectrum modeling and analysis. Med. Phys. 2016; 43(8): 4711-4717.
- 250 9. Knox R. Radiography and Radio-therapeutics Part 2: Radio-therapeutics. The Macmillan  
251 Company. New York 1919: 479.
- 252 10. U.S. Code of Federal Regulations Title 21, Part 1020: Performance Standards for Ionizing  
253 Radiation Emitting Products. Rev. 4/1/2019.  
254 <https://www.accessdata.fda.gov/scripts/cdrh/cfdocs/cfcfr/CFRSearch.cfm?FR=1020.30>
- 255 11. Frederick Holmes MD. Tuberculosis in the First World War. University of Kansas – School of  
256 Medicine. <http://www.kumc.edu/wwi/medicine/tuberculosis.html>
- 257 12. Williams FH. The Roentgen rays in Medicine and Surgery As an Aid in Diagnosis and as a  
258 Therapeutic Agent. The Macmillan Company. New York. 1903.
- 259 13. ICRP, 2012. ICRP Statement on Tissue Reactions / Early and Late Effects of Radiation in  
260 Normal Tissues and Organs – Threshold Doses for Tissue Reactions in a Radiation Protection  
261 Context. ICRP Publication 118. Ann. ICRP 41(1/2).
- 262 14. Balter S and Miller DL. Patient skin reactions from interventional fluoroscopy procedures.  
263 AJR. 2014; 202:W335-W342.
- 264 15. ICRP, 2013. Radiological protection in cardiology. ICRP Publication 120. Ann. ICRP 42(1).
- 265 16. Darby SC, Cutter DJ, Boerma M, et al. Radiation-related heart disease: Current knowledge  
266 and future prospects. Int J Radiat Oncol Biol Phys. 2010; 76(3):656-665.

- 267 17. Rosen II, Fischer TA, Antolak JA, et al. Correlation between lung fibrosis and radiation  
268 therapy dose after concurrent radiation therapy and chemotherapy for limited small cell  
269 lung cancer. *Radiology*. 2001; 221:614-622.
- 270 18. Stovall M, Smith SA, Langholz BM, et al. Dose to the contralateral breast from radiation  
271 therapy and risk of second primary breast cancer in the WECARE study. *Int J Radiat Oncol*  
272 *Biol Phys*. 2008; 15(4):1021-1030.
- 273 19. Werner-Wasik M, Yorke E, Deasy J, et al. Radiation dose-volume effects in the esophagus.  
274 *Int J Radiat Oncol Biol Phys*. 2010; 76(3):S86-S93.
- 275 20. Adams MJ, Dozier A, Shore RE, et al. Breast cancer risk 55+ years after irradiation for an  
276 enlarged thymus and its implications for early childhood medical irradiation today. *Cancer*  
277 *Epidemiol Biomarkers Prev*. 2010; 19(1):48-58.
- 278 21. Sahgal A, Chang JH, Ma L, et al. Spinal cord dose tolerance to stereotactic body radiation  
279 therapy. *Int J Radiat Oncol Biol Phys*. 2019; 1-13. doi.org/10.1016/j.ijrobp.2019.09.038
- 280 22. Benedict SH, Yenice KM, Followill D, et al. Stereotactic body radiation therapy: The report of  
281 AAPM Task Group 101. *Med. Phys*. 2010; 37(8):4078-4101.
- 282 23. Uniyal SC, Chatuverdi V, Sharma SD, et al. Patient dosimetry during interventional cardiac  
283 procedure in a dedicated catheterization laboratory. *Radiat. Prot. Dosimetry*. 2017;  
284 175(2):201-208.
- 285 24. Simpson S, Kay FU, Abbara S, et al. Radiological Society of North America expert consensus  
286 statement on reporting chest CT findings related to COVID-19. *J. Thorac. Imaging*. 2020
- 287 25. Tubiana M, Diallo I, Chavaudra J, et al. A new method of assessing the dose-carcinogenic  
288 effect relationship in patients exposed to ionizing radiation. A concise presentation of  
289 preliminary data. *Health Physics*. 2011; 100(3):296-299.



- 290 26. Tharmalingam H, Díez P, Tsang Y, Hawksley A, Conibear J, Thiruthaneeswaran N. Personal  
291 View: Low-dose Lung Radiotherapy for COVID-19 Pneumonia - The Atypical Science and the  
292 Unknown Collateral Consequence [published online ahead of print, 2020 Jun 10]. *Clin Oncol*  
293 (*R Coll Radiol*). 2020;S0936-6555(20)30236-3. doi:10.1016/j.clon.2020.06.002.
- 294 27. Fried C. The roentgen treatment of experimental pneumonia in the guinea-pig. *Radiology*.  
295 1941; 37, 197-202.
- 296 28. Glenn JC. Further studies on the influence of X-rays on the phagocytic indices of healthy  
297 rabbits. *J Immunol*. 1946; 53, 95-100.
- 298 29. Arenas M, Sabater S, Hernandez V, et al. Anti-inflammatory effects of low-dose  
299 radiotherapy. *Strahlenther Onkol*. 2012; 188:975-981.
- 300 30. Lara PC, Burgos J, and Macias D. Low dose lung radiotherapy for COVID-19 pneumonia. The  
301 rationale for a cost-effective anti-inflammatory treatment. *Clin. Transl. Radiat. Oncol*. 2020;  
302 23:27-29.
- 303